

# Functional morphology and light-gathering ability of podocopid ostracod eyes and the palaeontological implications

GENGO TANAKA\*

Department of Geoscience, Shizuoka University, 836 Ohya, Suraga-ku, Shizuoka 422–8529, Japan

Received January 2005; accepted for publication October 2005

The optical features of lateral ocelli of the eye were examined in 29 Recent species of the major ostracod group Podocopida using a theoretical morphological model. A cuticular lens–tapetum model was used for this purpose. Ray tracing was simulated on each model in order to assess the light-gathering abilities of the various forms of eyes. The results of computer simulations and morphospace analyses indicated that the light-gathering ability of the eye is dominantly affected by the thickness and curvature of the outer surface of the lens. On the basis of a combination of form and light-gathering ability, four eye types (LG1, LG2, MG, and HG) were recognized. The results of the phototactic experiment and the light intensity from each microhabitat were concordant with estimated scores on the light-gathering abilities using the theoretical models. Phylogenetic analyses and the fossil record indicate that the MG type is the most plesiomorphic, and that the other types derive from this. The present study also suggests that the optical structure that determines the light-gathering ability is closely related to the development of surface ornamentation on the valve. © 2006 The Linnean Society of London, *Zoological Journal of the Linnean Society*, 2006, 147, 97–108.

ADDITIONAL KEYWORDS: fossil record – morphospace – naupliar eye – optics – Ostracoda – Podocopa.

## INTRODUCTION

Since Exner's (1891) pioneering work, the geometrical optics of arthropod eyes has attracted considerable attention from functional morphologists. The functions of arthropod eyes have been interpreted from the viewpoint of their optical characteristics and uses (e.g. Clarkson & Levi-Setti, 1975; Land, 1976, 1980, 1981; Nilsson, Land & Howard, 1984; Nilsson, 1988, 1990; Warrant & McIntyre, 1993; Gál *et al.*, 2000). Although there are various types of arthropod eye, most studies of functional morphology have concentrated on compound eyes as a means of assessing their sensitivities and resolving powers.

The naupliar eye is one of the most common optical systems in crustacean arthropods. Ostracods are tiny bivalved crustaceans (average adult length approximately 1 mm) that are abundant in the fossil record (from at least the Ordovician onwards) and in a wide

range of aquatic environments at the present time (Fig. 1). The vast majority of the estimated 20 000-plus Recent ostracod species belong to the order Podocopida (subclass Podocopa), a group in which a naupliar (median) eye is often present but compound (lateral) eyes are absent. In podocopid ostracods, the cuticular lens of the naupliar eye is commonly preserved as part of the fossilized calcareous valves (Fig. 1) and therefore has been a popular subject of palaeoecological and palaeoenvironmental studies (Van Morkhoven, 1962; Benson, 1975, 1984; McKenzie & Peypouquet, 1984; Bonaduce & Danielopol, 1988; Kontrovitz & Myers, 1988; Puckett, 1991). However, little attention has been paid to the functional aspects of the naupliar eye.

Myers & Kontrovitz (1988) proposed an idealized model for the podocopid ostracod eye composed of a thin converging lens overlying the tapetum, which itself functions as a concave mirror. In their model, the radius of curvature of the tapetum was assumed to be equal to both the radius of the converging lens and the distance between the centre of the lens and the tapetal

\*E-mail: gngtnk@yahoo.co.jp

vertex. Their 'thin lens and tapetum model' can be regarded as equivalent to the 'thick lens in air system'. Myers & Kontrovitz (1988) calculated the  $f$  number (index of the brightness of the image constructed by the optical system) of an idealized podocopid ostracod eye by using the thin lens and tapetum model, and considered the podocopid ostracod eye to be very well adapted for dimly lit environments. However, they did not address the relationship between the shape and optical ability of the eye in actual specimens.

The present study analysed the relationship between the shape of the optical elements and the

light-gathering ability of the podocopid ostracod eye. For this purpose, ray-tracing simulations were performed on theoretical models, and morphometric analyses were carried out for actual specimens. The distance between the cuticular lens and the tapetum was also taken into consideration.

#### PODOCOPID OSTRACOD EYES

Two different types of photoreceptor occur in crustaceans, namely naupliar eyes and compound eyes. Podocopid ostracods possess only naupliar eyes. The eye system of podocopids typically consists of two lateral ocelli and a single ventral ocellus, but the ventral one is lacking in some species (Claus, 1891; Müller, 1894; Nowikoff, 1908; Rome, 1947; Elofsson, 1966; Andersson & Nilsson, 1981; Bonaduce & Danielopol, 1988). Each lateral ocellus sometimes attaches to a valve, and develops a cuticular lens on the valve itself (Fig. 2A). The pigment cup is connected with the cuticular lens by the connective tissue and surrounds the tapetum, reticular cells and lens cells. Some podocopids lack the lens cell (Fig. 2B). Each reticular cell generally has a single rhabdomere, and a pair of neighbouring rhabdomeres constitutes each rhabdom. The number of rhabdoms is different between species, totalling three to nine in each ocellus (Elofsson, 1966; Andersson & Nilsson, 1981). Because the pigment cup is usually buried in the calcified valve, forming an internal mould (Fig. 2B), its morphology potentially provides useful information on the visual system and taxonomy of fossil podocopids (Kontrovitz & Myers, 1984; Kontrovitz, 1985, 1987; Kontrovitz & Zhao, 1991; Kontrovitz & Slack, 1995; Kontrovitz & Puckett, 1998). Like other nervous systems, soft parts of the lateral ocelli, such as the pigment cup, tapetum, reticular cells, and lens cells, are formed inside the newly

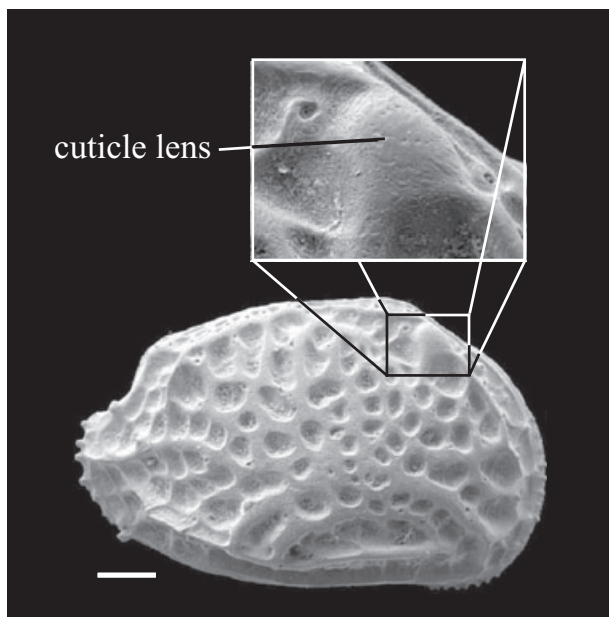


**Figure 1.** The podocopid ostracod *Aurila kiritsubo* Yajima, 1982; the right valve with a close-up of the cuticular lens. Scale bar = 100 µm.

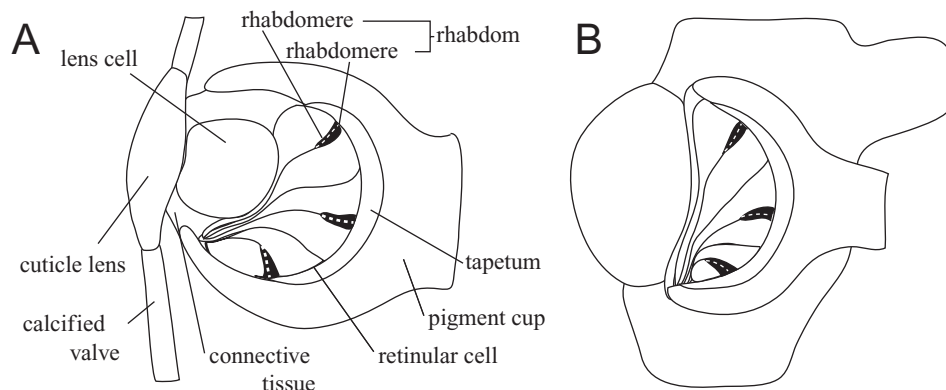


**Figure 2.** Idealized cross-sections showing the two possible ultrastructures of the podocopid lateral ocellus viewed from the anterior side. A, the pigment cup connects with the cuticular lens by connective tissue. B, the pigment cup is buried in the calcified valve, and the lens cell is degenerate.

secreted noncalcified carapace before ecdysis, which is followed by formation of the cuticular lens.

## MATERIAL AND METHODS

### MODELLING OF THE LATERAL OCELLUS

Because the lens cell has almost the same refractive index (1.37) as the reticular cells (1.35) (Andersson & Nilsson, 1981), variation in the lens cell does not significantly affect the optics of the system. The present model is represented by a simple optical system consisting of a cuticular lens and a tapetum. The size of the tapetum on the meridional cross-section is represented by its diameter,  $d$  (Fig. 3A). The front of the tapetum is assumed to be filled with a uniform medium of reticular cells with a refractive index of 1.35 (Andersson & Nilsson, 1981). The cuticular lens is set with its inner surface at a distance of  $e_2$  from the tapetum. The relative distance between the cuticular lens and the tapetum, or  $E_2$ , is defined as  $e_2/d$ .

The model of the cuticular lens can be defined if we specify the radius of curvature of its outer surface ( $r_1$ ),

the radius of curvature of the inner surface ( $r_2$ ), the thickness of the lens ( $e_1$ ), and a refractive index taken to be 1.64 (Fig. 3A). The present model is not intended for a lens with a concave outer surface, because such a lens forces light to diverge and does not work as an optical lens. The shape of the lens is defined by the following three parameters:  $R_1 = d/r_1$ , which represents the standardized curvature of its outer surface;  $R_2 = d/r_2$ , which represents the standardized curvature of the inner surface of the lens; and  $E_1 = e_1/d$ , which is the relative thickness of the cuticular lens. The lens aperture, as well as the shape of the lens, might be an important factor in considering the ability of the eye. However, the lens aperture is approximately equal to the diameter of the tapetum in actual podocopid eyes (Andersson & Nilsson, 1981: fig. 1). In the present model, the lens aperture is therefore set to be the same as the diameter of the tapetum when it is larger than  $d$ . Now we can define a theoretical model of the podocopid eye in terms of the four parameters,  $E_1$ ,  $E_2$ ,  $R_1$ , and  $R_2$ . Based on this model, computer simulations of ray tracing were performed using a program written in VISUAL BASIC.

In the present model, rays of incident light are received by a rectangular central rhabdom elongating from the inner surface of the tapetum towards the lens. As in the human eye, the rhabdom of the arthropod eye translates light into an electric stimulus by means of the depolarization on the cell membrane (Sandler & Kirschfeld, 1988). An electric signal is generated if a sufficient light stimulus is captured by the rhabdom. Because the rhabdom functions as a light guide, its diameter must be larger than a couple of micrometres, and it also needs to be long enough to receive the light stimulus (Land, 1981). In podocopid ostracods, the size of the rhabdom approximates to  $4 \times 15 \mu\text{m}$  (Andersson & Nilsson, 1981). The relative length of the rhabdom is set to be  $d/3$  and its thickness  $d/9$  (see Andersson & Nilsson, 1981). The rhabdom receives not only refracted light from the lens but also reflected light from the tapetum. In the present simulations, the light-gathering ability of the podocopid ostracod rhabdom was assessed by  $G = L_t/d/n$ , where  $L_t$  represents the sum of the total lengths of segments of rays passing through the rhabdom, and  $n$  is the sum of the number of rays of incident light.

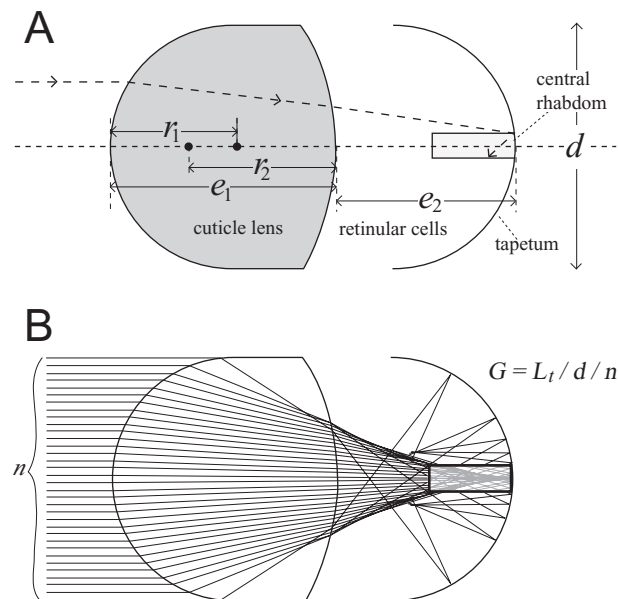


**Figure 3.** A, cuticular lens–tapetum model: bold dots in the lens represent the centre of the arc described by the outer and inner surface of the lens;  $r_1$ , the radius of curvature of the outer lens surface;  $r_2$ , the radius of curvature of the inner surface;  $e_1$ , the thickness of the lens;  $e_2$ , the distance between the lens and the tapetum;  $d$ , the diameter of a spherical mirror. B, an example of the computer simulation of ray tracing:  $L_t$ , the sum of the total lengths of segments of rays passing through the rhabdom (shown by the grey segments);  $n$ , the total number of rays of incident light.

### MORPHOSPACE ANALYSIS OF ACTUAL LATERAL OCELLI

To reveal the range of the four parameters in actual podocopid ostracods, 29 species belonging to seven podocopid families were studied. For each species, one adult specimen was examined (Table 1). All specimens were collected from various benthic localities from the intertidal zone to 20 m below the surface of the sea around the islands of Japan and Taiwan.

Table 1. Measured values of parameters and microhabitat for each species examined

Family	Species	$R_1$	$R_2$	$E_1$	$E_2$	$T_0$	$H_r$	$G$	$D$ (mm)	Microhabitat (water depth)
Cytheridae	<i>Cythere nishinipponica</i>	0.77	1.16	1.01	0.29	0.10	0.01	0.23	–	On calcareous algae (0 m)
	<i>Hemicythere ochotensis</i>	0.37	0.55	1.82	0.39	0.09	0.03	0.23	–	On sand bottom (0 m)
	<i>Laperousecythere yahtsensis</i>	0.36	0.59	1.60	0.44	0.07	0.03	0.23	–	On sand bottom (0 m)
	<i>Aurila corniculata</i>	0.66	0.39	1.19	0.51	0.07	0.02	0.23	–	On sand bottom (–4 m)
	<i>Aurila hataii</i>	0.40	1.12	1.85	0.61	–	–	0.23	20–25	On calcareous algae (–0.3 m)
	<i>Aurila kiritsubo</i>	0.64	1.02	1.52	0.44	0.07	0.05	0.23	–	On sand bottom (–9 m)
	<i>Aurila tosaensis</i>	0.47	0.74	1.31	0.36	0.08	0.04	0.23	–	On calcareous algae (–0.3 m)
	<i>Robstaurila ishizakii</i>	0.60	0.65	1.79	0.54	0.10	0.03	0.24	20–27	On calcareous algae (–0.3 m)
	<i>Caudites japonica</i>	0.73	0.59	1.39	0.38	0.14	0.02	0.23	–	On sand bottom (0 m)
	<i>Caudites cf. yambaensis</i>	0.79	0.98	0.80	0.40	0.04	0.02	0.23	–	On sand bottom (0 m)
Trachyleberididae	<i>Caudites</i> sp.	0.45	–0.18	1.08	0.74	0.08	0.03	0.23	–	On sea weed (–0.5 m)
	<i>Cornucoquimba tosaensis</i>	0.81	0.89	0.62	0.67	0.07	0.04	0.23	–	On sand bottom (–9 m)
	<i>Coquimba ishizakii</i>	0.52	0.57	0.91	0.42	0.08	0.01	0.23	–	On sand bottom (–10 m)
	<i>Hermanites transoceanica</i>	1.01	0.33	0.87	0.26	0.09	0.03	0.23	–	On sea grass (–0.5 m)
	<i>Trachyleberis scabrocuneata</i>	0.89	0.93	2.31	0.52	0.07	0.05	0.29	85	In sandy mud (–2 m)
	<i>Actinocythereis kisarazuensis</i>	0.85	–0.30	0.95	0.53	0.08	0.05	0.23	–	On sandy mud (–10 m)
	<i>Pistocythereis bradyformis</i>	1.12	1.18	1.20	0.93	–	–	0.36	–	In sandy mud (–20 m)
	<i>Bicornucythere bisanensis</i>	0.53	0.78	2.78	0.62	0.10	0.04	0.27	55–65	In mud (–2 m)
	<i>Hemicytherura cuneata</i>	0.42	0.16	1.27	0.68	0.05	0.02	0.23	20	On algae (–10 m)
	<i>Loxococoncha japonica</i>	0.84	1.55	0.98	0.49	0.05	0.02	0.22	–	On sea grass (–0.3 m)
Cytheruridae	<i>Loxococoncha uranouchiensis</i>	0.60	1.31	1.24	0.58	0.09	0.04	0.23	–	On sandy mud (–2 m)
	<i>Loxocorniculum mutsuense</i>	0.47	0.70	1.15	0.43	0.05	0.02	0.23	–	On calcareous algae (–0.3 m)
Xestoleberididae	<i>Xestoleberis kalibengensis</i>	0.18	–0.16	1.30	0.87	0.07	0.00	0.22	–	On calcareous algae (–0.5 m)
	<i>Xestoleberis hanaii</i>	0.14	–0.12	1.02	0.76	0.05	0.00	0.21	17–20	On calcareous algae (–0.5 m)
	<i>Xestoleberis setouchiensis</i>	0.18	–0.15	0.72	0.45	0.06	0.00	0.21	–	On sea weed (–0.1 m)
	<i>Xestoleberis</i> sp.	0.28	1.34	0.85	0.46	–	–	0.22	–	On calcareous algae (0 m)
Paradoxostomatidae	<i>Paradoxostoma pedale</i>	0.69	0.63	0.18	0.40	0.03	0.00	0.21	15	On sea weed (–0.1 m)
	<i>Paradoxostoma setoense</i>	0.46	0.31	0.29	0.80	0.02	0.00	0.22	–	On calcareous algae (–0.3 m)
	<i>Paradoxostoma setosum</i>	0.26	0.23	0.11	0.27	0.03	0.00	0.21	–	On sea weed (–0.3 m)



Measurements were made on thin sections of each specimen. Both newly collected and repository specimens were rinsed in 70% ethanol and then dehydrated in alcohol and embedded in epoxy resin. The cross-section of the embedded shell was made using a razor blade. The cut specimen was soaked, decalcified in 10% acetic acid for 12 h, washed, dried in air, and re-embedded in epoxy resin. Semi-thin sections (1  $\mu\text{m}$ ) were made using an ultramicrotome (Leica Ultracut) with glass knives. Each section was mounted on a slide and stained with 0.05% Toluidine Blue solution. The section was examined in a transmitted light microscope (Olympus BX41) under  $\times 400$  magnification. Micrographic images were taken using a digital camera (Nikon E4500). Radii of curvature of the cuticular lens and tapetum were calculated based on the coordinate data of three homologous points on their outer surfaces, which were digitized along each surface profile on the computer image using a program written in VISUAL BASIC. The thickness of the cuticular lens and the distance between the cuticular lens and the tapetum were also measured on the images. The light-gathering ability in each actual specimen was also estimated in the same manner with the theoretical model.

#### PHOTOTACTIC EXPERIMENTS USING SOME PODOCOPIDS

In order to clarify the relationship between the optical structure and the acceptable light intensity, phototactic experiments were carried out on seven species (Table 1, Fig. 4). First, an adult podocopid was put into a Petri dish paved with filter paper and filled with artificial sea water (2 ml, 34 psu) set on the stage of

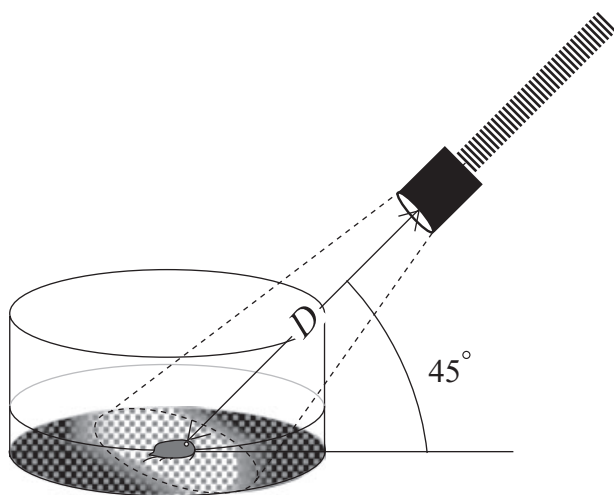


**Figure 4.** The setting for the phototactic experiments. A white fibre-optic illumination (150 W) from a halogen lamp was exposed to the podocopid ostracod at the distance of  $D$  and an angle of  $45^\circ$ .

the binocular microscope under diffuse room light conditions (188 lx). Subsequently, the ostracod was subjected to a directional light projected from a distance of 200 mm at an angle of  $45^\circ$ , with the light source being moved slowly towards the ostracod. The distance between the ostracod and the light source ( $D$ ) was measured when the ostracod began to escape. The light intensity (lx) was measured using an illuminometer (HIOKI 3423LUX HiTESTER) equipped with a silicon detector. Each experiment involved only one individual ostracod, although five individuals were tested in this way for each of the seven species selected.

## RESULTS

### MORPHOSPACE ANALYSIS

The values of  $G$  in relation to  $R_1$  and  $R_2$  at several values of  $E_1$  and  $E_2$  are given in a three-dimensional contour diagram (Fig. 5). When  $R_2 < 0$ , the inner surface of the lens is concave. A plano-concave meniscus lens is accommodated in the lower-left region of each morphospace. A prominent biconvex lens occurs in the upper-right area of the morphospace, whereas a plano-convex lens appears around the lower-right corner. A convex-concave meniscus lens occupies the upper-left region of each morphospace, but was not found in the specimens examined and is not illustrated in Figure 5. In the results, large  $G$  scores showing high light-gathering abilities were widely distributed in the large  $R_1$  region of a large  $E_1$  diagram (Fig. 5A, D, G). In the case of a large  $E_1$  value, a thick convex lens concentrates the rays of incident light on the focal point. In this condition, the light-gathering ability dominantly increases with increasing  $R_1$  rather than  $R_2$ . If the thickness of the lens is equal to the diameter of the tapetum (Fig. 5B, E, H), the light-gathering ability is generally low ( $G = 0.20\text{--}0.25$ ) regardless of the values of  $R_1$  and  $R_2$ . If the lens is much thinner than the diameter of the tapetum (Fig. 5C, F, I), an extremely low light-gathering ability ( $G < 0.15$ ) occurs in the biconvex and plano-convex regions, because these regions accommodate a lens with a very small diameter. In this case, contour lines run obliquely in the diagram, so that the light-gathering ability changes considerably with both  $R_1$  and  $R_2$ . However, the actual specimens utilized generally do not have such large values of  $R_2$ , except for a few species, and thus,  $R_2$  is not useful for determining  $G$  in the natural case. In summary, the significant parameters determining  $G$  values are  $R_1$  and  $E_1$ .

Subsequently, the values of light-gathering abilities estimated from the actual 29 species were compared with the calculated  $G$  values on  $E_1$ – $R_1$  morphospace when  $R_2 = 0.5$  and  $E_2 = 0.5$ . Most of the measured  $G$

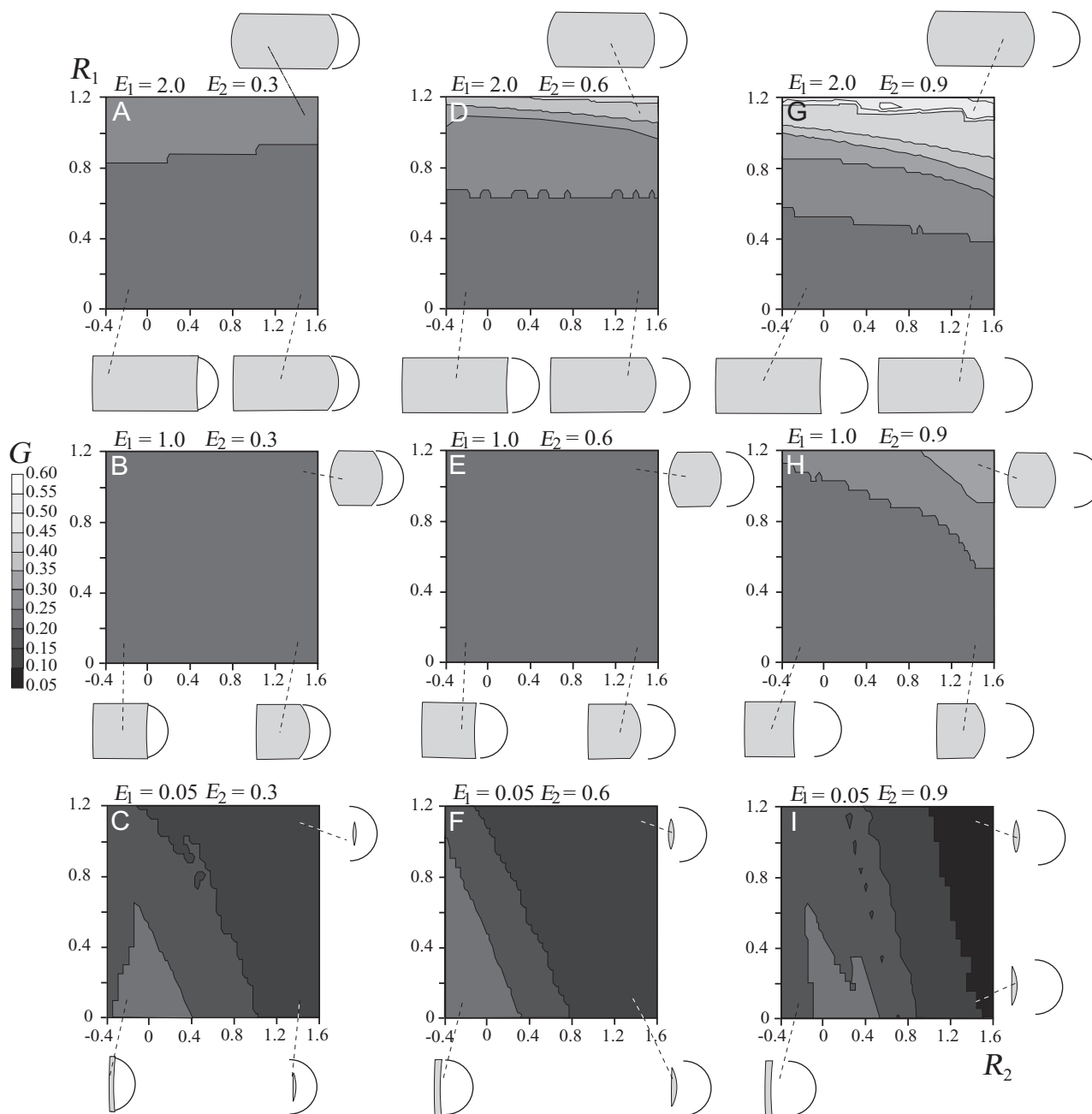


**Figure 5.** Nine selected three-dimensional contour diagrams showing the theoretical morphospace consisting of parameters  $R_1$ ,  $R_2$ , and  $G$ . The  $z$ -axis represents the  $G$  value corresponding to each combination of  $R_1$  and  $R_2$ , for  $E_1 = 2.0, 1.0$ , and  $0.05$ , and  $E_2 = 0.3, 0.6$ , and  $0.9$ . Selected theoretical models are given for the corresponding regions in the morphospace.

values were in accord with the calculated ones (Fig. 6). The result clearly indicates that the light-gathering ability of ostracod eyes dominantly depends on the standardized curvature of the outer lens surface ( $R_1$ ) and the relative thickness of the lens ( $E_1$ ). Therefore, the effects of  $R_1$  and  $E_1$  on  $G$  are particularly examined in the following discussion.

Referring to the values of  $G$ ,  $E_1$ , and  $R_1$ , on the basis of the species selected for this study, podocypid eyes

can be subdivided into four types (Fig. 7): (1) LG1 type, which has a very thin lens with low light-gathering ability ( $G = 0.21$ – $0.22$ ), and includes paradoxostomatids; (2) LG2 type, with a very small curvature of the outer surface of the lens and low light-gathering ability ( $G = 0.21$ – $0.22$ ), which is characteristically found in xestoleberidids; (3) MG type, with a wide range of  $E_1$  and  $R_1$  and medium light-gathering ability ( $G = 0.22$ – $0.24$ ), as seen in hemicytherids, loxocon-

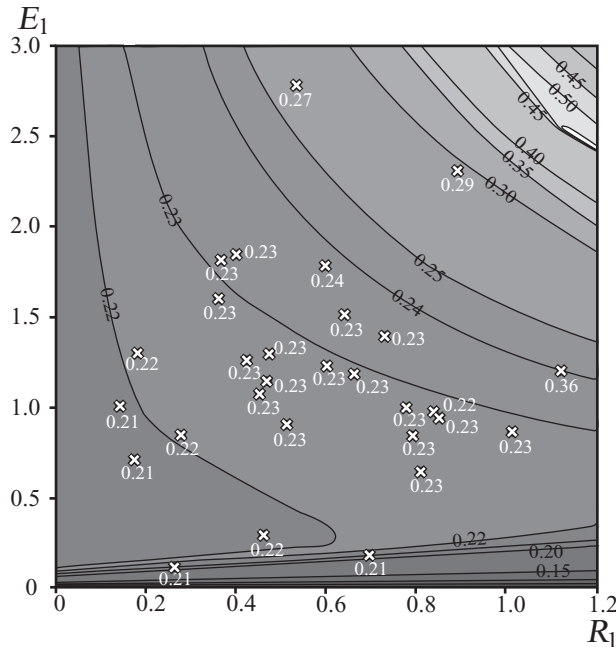


**Figure 6.** The estimated values of light-gathering abilities from measurements in 29 Recent podocopid ostracod species plotted on  $E_1$ - $R_1$  morphospace with the calculated value of  $G$  at  $R_2 = 0.5$  and  $E_1 = 0.5$ .

chids, cytherids, cytherurids, and trachyleberidids; and (4) HG type, with a wide range of  $E_1$  and  $R_1$  and high light-gathering ability ( $G = 0.27$ – $0.36$ ), as found in trachyleberidids.

#### PHOTOTACTIC EXPERIMENTS

All of the species examined did not respond to the flood light when  $D > 85$  mm (Table 1). The HG type of species, including two trachyleberidids, showed negative phototaxis when  $D = 85$  mm (Table 1). In this condition, the light intensity is smaller than 20 000 lx and is much weaker than that of a cloudy day (Land, 1981: table 3). The other types of ostracod showed strong positive phototaxis in the experimental condition of 27 mm =  $D < 85$  mm. The MG-type ostracods, which consist of hemicytherids and cytherurids, always showed negative phototaxis when  $D < 27$  mm. The LG2-type species, represented by xestoleberidids, were negatively phototactic if  $D < 20$  mm. All of the individuals belonging to the LG1 type, characteristically found in paradoxostomatids, began to escape the flood light at  $D = 15$  mm.

The results of the phototactic experiment show that the range of light intensity that ostracods disliked is well concordant with the present classification of eye types (LG1, LG2, MG, and HG). For example, the HG-type species were affected by a weaker light more than

the MG species were. This fact indicates that the  $G$  values estimated from the optical structure are appropriate for evaluating the sensitivity of the ostracod eye.

## DISCUSSION AND CONCLUSIONS

### PHOTOENVIRONMENTS AND PODOCOPID EYES

Myers & Kontrovitz (1988) estimated the light-gathering ability of podocopid ostracod eyes based on a simple model and suggested that the podocopid ostracod eye is optimized for dimly lit environments because of their low  $f$  numbers. However, their model consists of a lens directly attached to the hemispherical tapetum and therefore the focal length must be abridged by the reflection on the tapetum, causing an extremely low  $f$  number. In addition, Myers & Kontrovitz (1988) did not assess the effect of the size and shape of the lens on the light-gathering ability of the eye. The results of the present analysis clearly indicate that there are various forms of light-gathering ability in podocopid ostracod eyes, on account of the fact that the structure of the optical system is considerably different between species. The evaluation of the light-gathering ability in terms of morphological features of the optical system was supported by the results of the phototactic experiments undertaken.

These results have important implications for interpreting the environmental distribution and significance of types of podocopid eye. Additional information correlating each eye type with the light intensity of the experimental microhabitat further supports these interpretations.

To elucidate further the light-dependent distribution of podocopid eyes, the relationship between the total irradiance of each microhabitat and light-gathering ability has been analysed (Fig. 8). Total irradiance is known to decline with an increase in water depth (Jerlov, 1968). In the present study, the total irradiance of each microhabitat was estimated using published depth–irradiance data (Jerlov, 1968: table 21) based on water depth data (Table 1). Among the species studied herein, three trachyleberids, namely *Trachyleberis scabrocuneata* (Brady, 1880), *Pistocythereis bradyformis* (Ishizaki, 1968) and *Bicor-nucythere bisanensis* (Okubo, 1975), are burrowers and, therefore, must live in a darker environment than the adjacent open water. For *T. scabrocuneata* and *B. bisanensis*, the experimental data were converted (*T. scabrocuneata*, approximately 12 000 lx; *B. bisanensis*, approximately 15 000 lx) into irradiance based on Land's (1981) formula. In the case of *P. bradyformis*, for which no experimental data could be obtained, the water depth data were applied directly.

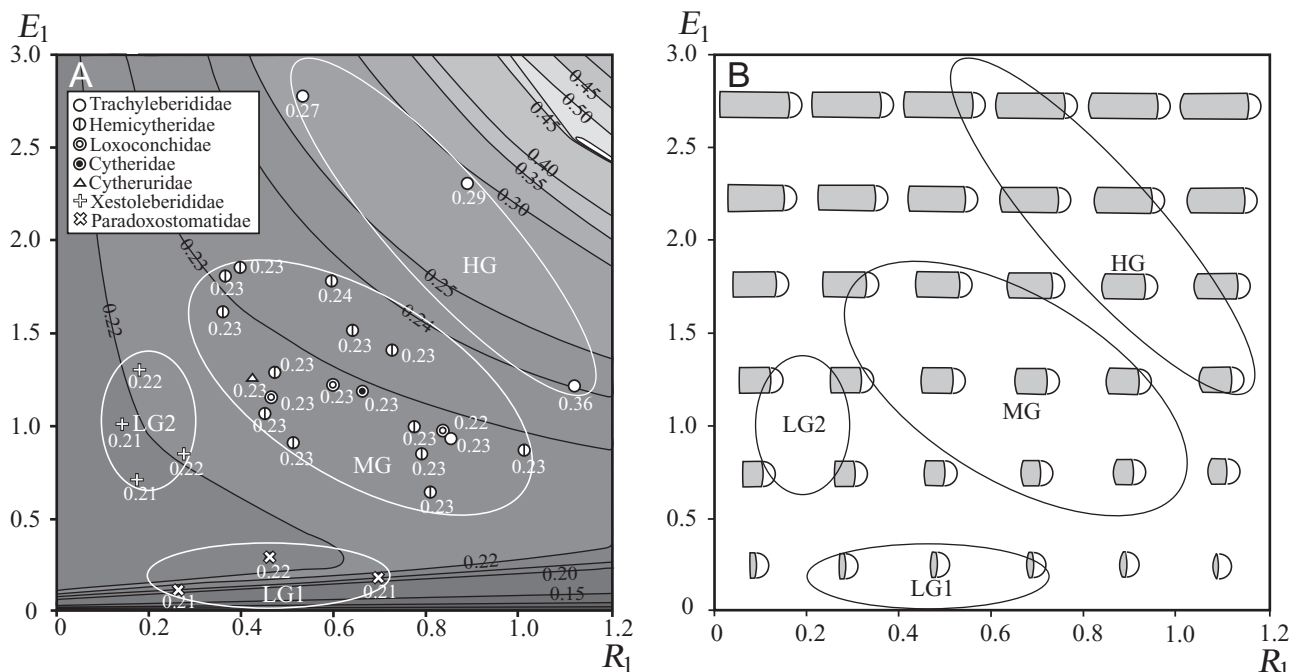


**Figure 7.** A, measurements of the four types of podocopid species (LG1, LG2, MG, and HG) plotted on Figure 6. B, theoretical models of possible podocopid ostracod eyes accommodated in the morphospace.

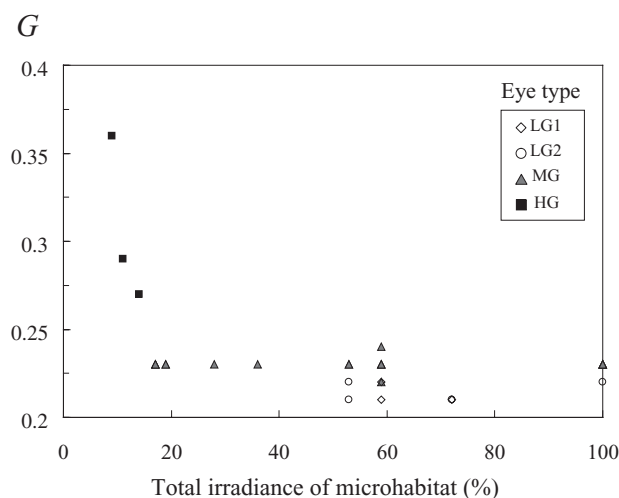


**Figure 8.** The relationship between the total irradiance of the microhabitat (%) of each species (where the total irradiance at the sea surface is 100%) and the light-gathering ability of eyes ( $G$ ).

The results (Fig. 8) indicate that the eyes belonging to the MG type tend to occur in a somewhat wide range of irradiance, but LG1 and LG2 types occur in high irradiance regions. The HG type occupies lower irradiance environments than the other types. The present study revealed that podocopid ostracods

possess eyes that are adapted to different light conditions.

#### PHYLOGENETIC CONSIDERATIONS AND FOSSIL RECORDS OF PODOCOPID EYES

Among the various types recognized, the eyes belonging to the MG type tend to be located at the central region of the morphospace, which describes the possible distribution of each eye shape and its light-gathering ability on the  $E_1$  and  $R_1$  space (Fig. 7). The LG types are situated on the opposite side to the HG type across the MG-type region. The spatial distribution of each eye type in the morphospace suggests that any of the HG, LG1 and LG2 types can derive from the MG type by altering the shape slightly. The distribution in the morphospace is also concordant with a phylogenetic relationship between podocopid ostracods proposed by Yamaguchi (2003), inferred from 18S rDNA nucleotide sequences (Fig. 9). According to this molecular tree, the stem groups of the Cytheroidea are expected to lack a cuticular lens. The most-parsimonious reconstruction of character evolution of the eye type based on this tree indicates that the MG type is the most plesiomorphic. The Eucytheridae, which is the sister group of all species studied but was not utilized in this study, is known to have a lens with a medium thickness and moderate radius of curvature of the outer surface (Witte, 1993), and thus appears to



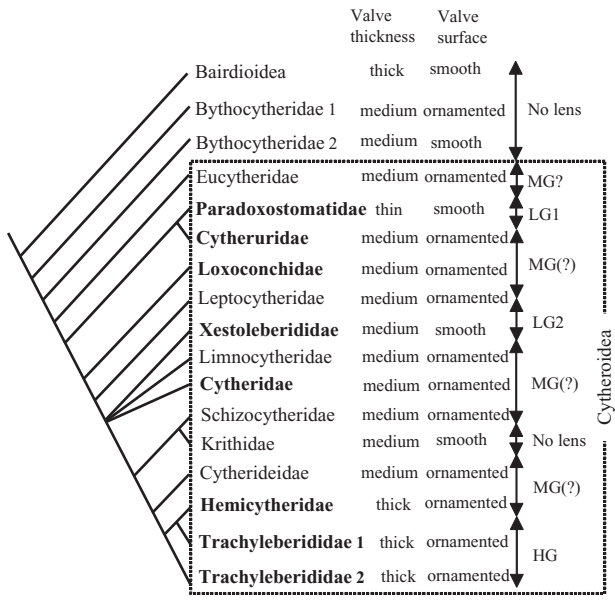


**Figure 9.** Character state distribution of podocopids on a phylogenetic tree proposed by Yamaguchi (2003). The families not shown in bold face were not examined in this study, and estimations of their eye types were mainly based on the figures and descriptions of the cuticular lens by Benson *et al.* (1961) and Van Morkhoven (1963).

belong to the MG type. The LG1 type is considered to have derived from the MG type by acquiring a very thin lens (Figs 7, 9). On the other hand, the LG2 type of eye probably evolved via a flattening of the outer lens surface of the ancestral MG form. Because the LG1 and LG2 eye types seem to have evolved independently (Fig. 9), their low light-gathering ability is interpreted as homoplasious. The HG eye type is characteristic of a paraphyletic family, the Trachyleberididae (Fig. 9). Figure 9 indicates either the possibility of homoplasy of the HG type of the Trachyleberididae or evolutionary reversal of the MG type of the Hemicytheridae. In either case, the HG type probably derived from the MG type by making the lens thicker and more convex.

The distribution of eye types throughout geological time, based on the stratigraphical ranges of ostracod families, also provides information on the evolution of podocopid eyes (Fig. 10). As for the families that were not utilized in the present study, eye types have been categorized based on literature information (Benson *et al.*, 1961; Van Morkhoven, 1963).

Fossil evidence demonstrates that among cytheroidean families, the diversification of eyes occurred in the Mesozoic, and that the MG type was the first eye to evolve following ostracod groups having lens-less eyes, a sequence predicted by molecular phylogeny. Based on molecular phylogeny and fossil data, LG1 and LG2 types seem to have evolved independently

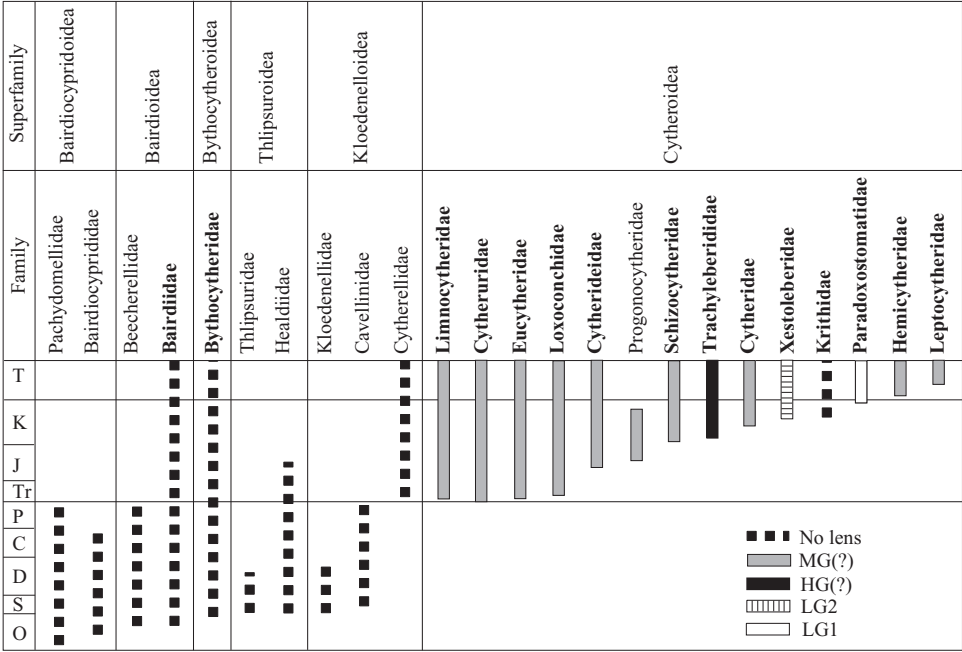


**Figure 10.** Stratigraphic ranges of marine podocopid ostracods [based on Whatley, Siveter & Boomer (1993) and Whatley & Boomer (2000)]. Note: Athersuch, Horne & Whittaker (1989) recognized the Bythocytheroidea as an independent superfamily, but Whatley *et al.* (1993) did not. The families dealt with in Figure 9 are shown in bold face.

from the MG type in the Mesozoic. The relationship between the HG type of the Trachyleberididae and the MG type of the Hemicytheridae remains uncertain, because the position of the Progonocytheridae is controversial. Overall, these data strongly lead to the conclusion that the HG, LG1, and LG2 types are derived from the MG type.

#### MORPHOLOGICAL CONSTRAINTS ON PODOCOPID EYES

As mentioned above, light-gathering ability is dominantly affected by the standardized curvature of the outer lens surface and relative thickness of the lens. Bonaduce & Danielopol (1988) reported morphological relationships between lens shape and carapace characters in xestoleberidids. According to those authors, the convex lens was characteristically found in a prominently ornamented valve, while the plano lens was restricted to the species lacking ornamentation. They also found that all of the interstitial species that had a degenerated eye possessed thin and smooth valves. Bonaduce & Danielopol (1988) suggested that valve thickness and ornamentation generally constrain the development of the lens in podocopid ostracods.

To test their hypothesis, I analysed the relationship between the relative valve thickness and the relative thickness of the lens, and the relationship between the relative height of the ridge of the ornament and the standardized curvature of the outer lens surface. The relative valve thickness ( $T_v$ ) was represented by the height of the nearest neighbouring ridge to the eye divided by the height of the valve. The relative height of the ridge ( $H_r$ ) was estimated by measuring the difference between the height of the ridge and the depth of the sulcus in the neighbouring region to the eye, and dividing this by the height of the valve.

As a result, a positive correlation was recognized between  $T_v$  and  $E_1$  at the 1% level of significance (Fig. 11A). This fact indicates that a stout valve tends to have a thick lens, whereas a lens formed in a thin valve generally lacks thickness. This result appears to be reasonable from the viewpoint of mechanical strength. A flimsy valve seems to be too fragile to support a massive lens.

On the other hand, all of the species bearing valve ornament have convex lenses with  $R_1$  values  $> 0.3$ . A flat lens in an ornamented valve cannot function properly because the rays of light incident towards the lens are refracted and/or reflected in various directions by the protruding ridges beyond the outer lens surface. In addition, Okada (1981, 1982) reported that the non-calcified prototype of the ornamentation is formed prior to the construction of the lens in podocopids. This fact suggests that the secretion of ample cuticular

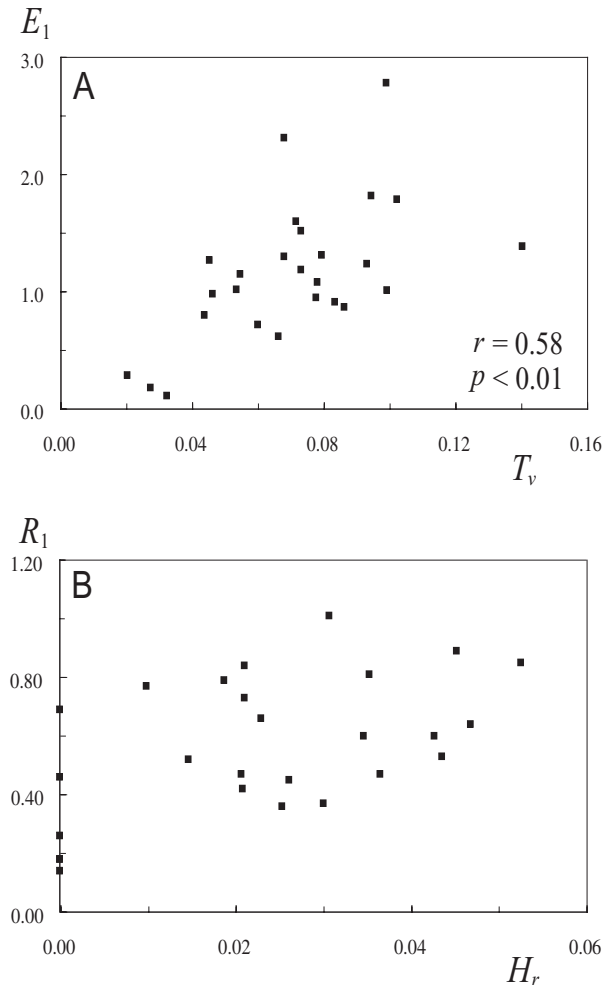


**Figure 11.** A, the relationship between the relative valve thickness ( $T_v$ ) and the relative thickness of the lens ( $E_1$ );  $r$ , correlation coefficient;  $P$ , significance level of the correlation. B, plots of the standardized curvature of the outer lens surface ( $R_1$ ) against the relative height of the ridge ( $H_r$ ).

materials for the formation of the ornament allows the incipient lens to swell enough to construct a large curvature of the outer lens surface. These may be reasons why ornamented podocopid ostracods tend to have a more convex lens than smooth ones (Fig. 11B). Indeed, the HG-type species living in a dimly lit environment possess ornamented valves, whereas the LG1- and LG2-type species living in a strongly lit environment have smooth valves (Figs 8, 9). These facts suggest that losing ornament in order to make a flat lens is an efficient tactic for life in environments with strong light. The most-parsimonious reconstruction of character evolution on the phylogenetic tree shows that several evolutionary reversals from ornamented to smooth independently occurred in podocopid ostracods (Fig. 9). This interpretation suggests that a smooth

valve can readily evolve from an ornamented ancestor with the MG type of eye.

On the other hand, a thick valve is restricted to the clade consisting of the Hemicytheridae and Trachyleberididae, implying a phylogenetic constraint. According to my observations, a shelf-slope trachyleberidid species, *Acanthocythereis dunelmensis* (Norman, 1865), has a heavily calcified and ornamented valve and a thick prominent convex lens, which is probably plotted in the HG region of the morphospace proposed in this study. However, with the exception of trachyleberidid species, podocopid ostracods collected from the Japan Sea (< 253 m depth) have thin and smooth valves and degenerate eyes. The bathyal podocopid ostracods possessing flimsy valves may have failed to evolve thicker valves because of the phylogenetic constraint that did not permit the evolution of a massive lens.

#### PODOCOPID EYES AND GEOLOGICAL EVENTS

During the Palaeozoic, the ubiquitous 'palaeocopid' ostracods occupied a wide range of aquatic environments, from near-shore to outer shelf. On the other hand, as illustrated by Siveter (1984), podocopid ostracods tend to be dominant in deeper environments, such as lower shelf and shelf-slope settings. Some 'palaeocopid' ostracods had a cuticular lens (Kesling & Chilman, 1987: fig. 5), but as far as is known, all of the podocopids lacked a lens. The Late Palaeozoic extinction of the 'palaeocopids' and the eustatic rise in sea level in the Triassic could possibly have opportunistically opened up various 'light environments' or new niches to podocopid ostracods, which may have been a strong selection pressure for the development of their cuticular lenses. The cytheroidean podocopids are considered by some to have derived from the bythocytheroideans in the Late Palaeozoic, and many of the Triassic cytheroideans have been recorded from shallow shelf and marginal marine environments (Whatley & Boomer, 2000). Moving into shallow environments, the MG type of eye might have rapidly evolved within the medium-thick-shelled and ornamented cytheroideans. Ostracod radiations towards stronger or dimmer lit environments required the development of more specialized cuticular lenses, by changes in valve thickness and ornamentation.

In conclusion, the present study indicates that the naupliar eye has various light-gathering abilities depending on the parameters of the lens shape. The morphological diversity of the podocopid eye is postulated to result from the interplay between phylogenetic constraints and ecological demands on the animal. An integrated approach of optics and phylogenetics will provide a better understanding of the evo-

lution of the podocopid eye in the framework of constructional morphology (Seilacher, 1970).

#### ACKNOWLEDGEMENTS

The author wishes to thank T. Ubukata, D. J. Siveter and A. R. Parker for critically reviewing the manuscript and invaluable comments, N. Ikeya, M. Kontrovitz and A. Tsukagoshi for their helpful advice, and participants in the workshop on 'Fossils and Morphology' held in the Misaki Marine Biological Station in 2000 for constructive discussions. Thanks are due to K. Tazaki for the use of the ultramicrotome, and to the Research Institute of Tropical Biosphere, University of Ryukyus, for their support with sample collecting during fieldwork. This study has been partly subsidized by the Grant-in-Aid for JSPS Fellows (no. 08594 in 2003).

#### REFERENCES

- Andersson A, Nilsson DE. 1981. Fine structure and optical properties of an ostracode (Crustacea) nauplius eye. *Proto-plasma* **107**: 361–374.
- Athersuch J, Horne DJ, Whittaker JE. 1989. *Marine and brackish water ostracods (superfamilies Cypridacea and Cytheracea): keys and notes for the identification of the species*. Leiden: The Linnean Society of London and the Estuarine and Brackish-water Sciences Association.
- Benson RH. 1975. Morphological stability in Ostracoda. *Bulletin of American Paleontology* **65**: 13–46.
- Benson RH. 1984. Estimating greater paleodepths with ostracodes, especially in past thermosperic oceans. *Palaeogeography, Palaeoclimatology, Palaeoecology*. **48**: 107–141.
- Benson RH, Berdan JM, Van Den Bold WA, Hanai T, Hessland I, Howe HV, Kesling RV, Levinson SA, Reymont RA, Moore RC, Scott HW, Shaver RH, Sohn IG, Stover LE, Swain FM, Sylvester-Bradley PC. 1961. Systematic descriptions. In: Moore RC, ed. *Treatise on invertebrate paleontology, Part Q, Arthropoda 3*. Lawrence: Geological Society of America and University of Kansas Press, Q99–Q421.
- Bonaduce G, Danielopol DL. 1988. To see and not to be seen: the evolutionary problems of the Ostracoda Xestoleberididae. In: Hanai T, Ikeya N, Ishizaki K, eds. *Evolutionary biology of Ostracoda, its fundamentals and applications*. Tokyo: Kodansha, 375–398.
- Brady GS. 1880. Report on the Ostracoda dredged by H.M.S. Challenger, during the years 1873–1876. Report on the scientific results of the voyage of H.M.S. Challenger. *Zoology* **1**: 1–184.
- Clarkson ENK, Levi-Setti R. 1975. Trilobite eyes and the optics of Des Cartes and Huygens. *Nature* **254**: 663–667.
- Claus C. 1891. Das Medianauge der Crustaceen. *Arbeiten aus dem Zoologischen Institut der Universität zu Wien* **9**: 225–266.
- Elofsson R. 1966. The nauplius eye and frontal organs of the non Malacostraca (Crustacea). *Sarsia* **25**: 1–128.

- Exner S. 1891.** *Die physiologie der facettiirten augen von kreb- sen und insecten*. English translation by Hardie RC. 1988. *The physiology of the compound eyes of insects and crusta- ceans*. New York: Springer.
- Gál J, Horváth G, Clarkson ENK, Haiman O. 2000.** Image formation by bifocal lenses in a trilobite eye? *Vision Research* **40**: 843–853.
- Ishizaki K. 1968.** Ostracodes from Uranouchi Bay, Kochi Prefecture, Japan. *Science Reports of the Tohoku University, Second Series, Geology* **40**: 1–45.
- Jerlov NG. 1968.** *Optical oceanography*. Amsterdam: Elsevier.
- Kesling RV, Chilman RB. 1987.** Dimorphic Middle Devonian paleocopan Ostracoda of the Great Lakes region. *Museum of Paleontology, University of Michigan, Papers on Paleontology* **25**: 1–227.
- Kontrovitz M. 1985.** Ocular sinuses in some genera of the ostracode Family Trachyleberididae. *Transactions Gulf Coast Association of Geological Societies* **35**: 425–430.
- Kontrovitz M. 1987.** Ocular sinuses in some modern and fos- sil species of *Echinocythereis* (Ostracoda). *Micropaleontology* **33**: 93–96.
- Kontrovitz M, Myers JH. 1984.** A study of the morphology and dioptrics of some ostracode eyespots. *Transactions Gulf Coast Association of Geological Societies* **34**: 369–372.
- Kontrovitz M, Myers JH. 1988.** Ostracode eyes as paleoen- vironmental indicators: physical limits of vision in some podocopids. *Geology* **16**: 293–295.
- Kontrovitz M, Puckett TM. 1998.** Ocular shell structures in some Cretaceous trachyleberid Ostracoda. *Micropaleontol- ogy* **44**: 201–206.
- Kontrovitz M, Slack JM. 1995.** Ocular shell structures in some loxoconchid Ostracoda. *Micropaleontology* **41**: 369–374.
- Kontrovitz M, Zhao Y. 1991.** Stereoscopic study of the ocular sinuses of some Ostracoda. *Revista Española de Micropale- ontologia* **23**: 27–35.
- Land MF. 1976.** Superposition images are formed by reflection in the eyes of some decapod crustacea. *Nature* **263**: 764–765.
- Land MF. 1980.** Compound eyes: old and new optical mecha- nisms. *Nature* **287**: 681–686.
- Land MF. 1981.** Optics and vision in invertebrates. In: Atrium H, ed. *Comparative physiology, evolution of vision in inver- tebrates B: invertebrate vision centers and behavior I*. Berlin: Springer, 471–593.
- McKenzie KG, Peypouquet JP. 1984.** Oceanic paleoenviron- ment of the Miocene Fyansford Formation from Fossil Beach, near Mornington Victoria interpreted on the basis of Ostra- coda. *Alcheringia* **8**: 291–303.
- Müller GW. 1894.** *Die Ostracoden des Golfes von Neapel und der angrenzenden Meeres-abschnitte*. Berlin: Verlag von R. Friedländer & Sohn.
- Myers JH, Kontrovitz M. 1988.** Geometrical optics of some ostracod eyes. In: Hanai T, Ikeya N, Ishizaki K, eds. *Evolu- tionary biology of Ostracoda, its fundamentals and applica- tions*. Tokyo: Kodansha, 187–193.
- Nilsson DE. 1988.** A new type of imaging optics in compound eyes. *Nature* **332**: 76–78.
- Nilsson DE. 1990.** From cornea to retinal image in inverte- brate eyes. *Trends in Neurosciences* **13**: 55–64.
- Nilsson DE, Land MF, Howard J. 1984.** Afocal apposition optics in butterfly eyes. *Nature* **312**: 561–563.
- Norman AM. 1865.** Report on the Crustacea. *Transactions of the Natural History Society of Northumberland, Durham and Newcastle-Upon-Tyne* **1**: 12–29.
- Nowikoff M. 1908.** Über den Bau des Medianauges der Ostra- coden. *Zeitschrift für Wissenschaft Zoologie* **91**: 81–92.
- Okada Y. 1981.** Development of cell arrangement in ostracod carapaces. *Paleobiology* **7**: 276–280.
- Okada Y. 1982.** Structure and cuticle formation of the reticu- lated carapace of the ostracode *Bicornucythere bisanensis*. *Lethaia* **15**: 85–101.
- Okubo I. 1975.** *Callistocythere pumila* Hanai, and *Legmi- nocythereis bisanensis* sp. nov., in the Inland Sea, Japan (Ostracoda). *Proceedings of the Japanese Society of System- atic Zoology* **11**: 23–31.
- Puckett TM. 1991.** Absolute paleobathymetry of Upper Cretaceous chalks based on ostracodes – evidence from the Demopolis Chalk (Campanian and Maastrichtian) of the northern Gulf Coastal Plain. *Geology* **19**: 449–452.
- Rome R. 1947.** *Herpetocypris reptans* Baird (Ostracoda), étude morphologique et histologique. I. Morphologie externe et système nerveux. *Cellule* **51**: 51–152.
- Sandler C, Kirschfeld K. 1988.** Light intensity controls extracellular  $Ca^{2+}$  concentration in the blowfly retina. *Natur- wissenschaften* **77**: 256–258.
- Seilacher A. 1970.** Arbeitskonzept zur Konstruktions-Mor- phologie. *Lethaia* **3**: 393–396.
- Siveter DJ. 1984.** Habitats and modes of life of Silurian ostracodes. In: Bassett MG, Lawson JD, eds. *Autecology of Silurian organisms, Special Papers in Palaeontology* 32. London: The Palaeontological Association, 71–85.
- Van Morkhoven FPCM. 1962.** *Post-Palaeozoic Ostracoda: their morphology, taxonomy and economic use, Vol. 1, Gen- eral*. New York: Elsevier.
- Van Morkhoven FPCM. 1963.** *Post-Palaeozoic Ostracoda: their morphology, taxonomy and economic use, Vol. 2, Generic description*. New York: Elsevier.
- Warrant EJ, McIntyre PD. 1993.** Arthropod eye design and the physical limits to spatial resolving power. *Progress in Neurobiology* **40**: 413–461.
- Whatley RC, Boomer ID. 2000.** Systematic review and evo- lution of the early Cytheruridae (Ostracoda). *Journal of Micropalaeontology* **19**: 139–151.
- Whatley RC, Siveter DJ, Boomer ID. 1993.** Arthropoda (Crustacea: Ostracoda). In: Benton MJ, ed. *The fossil record* 2. London: Chapman & Hall, 343–356.
- Witte LJ. 1993.** Pacific ostracods on West African beaches; a case of anthropogenic faunal contamination by shipping. In: Witte LJ, ed. *Taxonomy and origin of modern West African shallow marine Ostracoda*. Amsterdam: Academische Pers BV, 145–164.
- Yajima M. 1982.** Late Pleistocene Ostracoda from the Boso Peninsula, Central Japan. *Bulletin of the University Museum, University of Tokyo* **20**: 141–227.
- Yamaguchi S. 2003.** Morphological evolution of cytherocopine ostracods inferred from 18S ribosomal DNA sequences. *Jour- nal of Crustacean Biology* **23**: 131–153.